APPLICATION OF DETECTION PROBABILITIES IN THE IDC GLOBAL PHASE ASSOCIATION PROCESS

Tormod Kværna[1], Frode Ringdal[1], and Jeffrey Given[2]

NORSAR[1] and Comprehensive Nuclear-Test-Ban Treaty Organization[2]

Sponsored by the Comprehensive Nuclear-Test-Ban Treaty Organization

Award No. 2010-1445

ABSTRACT

The Global Association (GA) process at the International Data Centre (IDC) is an automated procedure that associates detections by stations in the International Monitoring System (IMS) in order to form event hypotheses. These hypotheses will later be reviewed by analysts before the Reviewed Event Bulletin (REB) is issued. We have begun investigating ways to improve the GA process for seismic data, in particular by incorporating amplitude data and station detection probabilities in the automatic process. We build on a previous study which has provided regional detection capability estimates for individual primary and auxiliary IMS stations, and use these estimates to develop and test various consistency measures. The purpose of these measures is to provide a means to assess the validity of seismic events automatically defined in the Standard Event Lists (SEL1, SEL2 and SEL3) and assess the consistency of individual phases associated with such events. By feeding the results of such assessments back into the GA procedure, we anticipate that the results of the global association can be iteratively improved.

A candidate SEL event is a group of automatically associated phases from IMS stations that satisfies certain predefined criteria for defining an event. For each such event an estimated origin time, hypocenter, a list of detecting stations and detected phases, phase arrival times and an average event magnitude as well as individual station magnitudes are given. Our basic approach is to make the hypothetical assumption that each such candidate event is real and correctly located. Using the regionalized station detection thresholds, we have the basis for calculating the station detection probability for events at that location as a function of event magnitude. By taking into consideration the actual pattern of detecting and non-detecting stations for the candidate event as listed in the SEL, we can therefore estimate a maximum-likelihood (MLE) magnitude for the hypothetical event. Based on this magnitude estimate, we then calculate, for each station, its probability of detection. By ranking the stations according to their detection probability, we can assess which stations are likely to detect or not detect this hypothetical event. We can then compare these probabilities to the actually observed phase list for the event as given in the SEL, and identify any inconsistencies

The single most important criterion for accepting a candidate SEL event is clearly the number of detecting stations that have been associated with the event. If this number is above a certain threshold, the event is accepted, perhaps with a suggestion to the analyst that one or more low probability phases be considered for deletion. Our approach therefore focuses on events with few (typically six or fewer) associated detecting stations. In such cases, we need to carry out several tests, and these tests are still under development. One promising approach is to take as starting point the number of *non-detecting* primary stations which have a higher detection probability than the *n'th best detecting* station (*n=1,2,3…).* For example, if the three primary stations with the highest detection probability are in fact associated with the event, then we would very likely accept the event, with a possible explanatory comment to the analyst. Other supplementary approaches are being considered.

An important consideration is to be able to identify whether or not a non-detecting station has actually been in operation at the expected time of detection. We accomplish this by making use of the continuous threshold monitoring (TM) system which is in operation at the IDC. The TM system calculates a threshold for each primary station at any point in time where data from that station is available, and therefore provides a reliable indication of the station's operational status. This paper presents some case studies illustrating various aspects of our approach.

OBJECTIVE

The objective of this project is to investigate various approaches to assessing the validity of seismic events defined through automatic phase association at the IDC. This includes the following:

- Develop and test various consistency measures for individual phases associated with a seismic event, using in particular the dynamic phase information (i.e., amplitudes or magnitudes).
- Define 'consistency indices' for each associated phase, and determine empirically a threshold for these indices in order to accept or reject a phase in the event definition.
- In this process, make use of the detection parameters of each station associated with the event as well as the information from non-detecting stations (i.e., stations not listed as associated with the event).

Our approach focuses on how to check individual phases of associated events after GA has been performed and magnitudes have been calculated (e.g., after SEL3). However, in principle such checks could be applied at any point in the phase association procedure, with feedback to GA for reprocessing as appropriate.

The study presented here is a first attempt to develop and test various consistency measures. They can be used individually or in combination. One important application is to provide the analyst with a summary of the consistency measurements for each individual event candidate. This would help in determining the most likely phases to delete or add in a possible revised solution.

RESEARCH ACCOMPLISHED

Estimating regionalized detection thresholds

The database for this study comprises automatic and reviewed event lists produced by the IDC from 1999 to present. The automatic event lists comprise SEL1, SEL2 and SEL3. The reviewed event lists comprise the REB and the late event bulletin (LEB). The LEB contains the REB events plus reviewed events that are real, but do not fulfil the formal event definition criteria. The work described in the following is an extension of the work by Kværna et al. (2009).

The event lists referenced above are based mainly on data from the primary and auxiliary seismic stations. However, observations from hydroacoustic and infrasonic stations are associated with some of the events. Although these two technologies are important components of the monitoring systems, the present project does not cover the analysis of hydroacoustic and infrasound data.

In order to obtain regionalized detection thresholds, we divide the events into a binned global grid system and investigate various ways to estimate the station detection threshold for each IMS station within each geographical bin. Clearly, there is a tradeoff between the grid density and the accuracy with which we can estimate the thresholds. In many bins, there will be few or none events, and in such cases a generic (average) threshold will be applied. It is important to make use of all available information, and for this reason, we have investigated three different estimation algorithms applied to each specific target area.

In the following discussion, we will illustrate the procedure for estimating station detection thresholds by presenting a specific example of a station/source region combination. As shown in Figure 1, we consider one station (ARCES) and a specific source area, in this example in China (the region within 1.5 degrees of 32^{o}N, 104^{o}E). Our purpose is to estimate the station detection threshold for events from this limited source area. From the REB, we obtain a large number of events, some detected by ARCES, some not detected by this station. Each event has reference network body-wave magnitudes, both conventional so-called generalized $m_b$values (Murphy and Barker, 2003) which we denote mb1, and MLE estimates. We have used the MLE magnitudes (mb1MLE) reported in the REB for reference event body-wave magnitude in this study.

Method 1

A commonly used method for threshold estimation is the approach described by Ringdal (1975). We will denote this approach *Method 1*. In this approach, the number of detections and non-detections in each magnitude bin is counted, and a cumulative Gaussian distribution curve is then fitted to the ensemble of observed detection percentages by maximum likelihood. The detection threshold m_t is considered to be a normally distributed random variable.

The probability *P(m)* of detecting an event of magnitude m at an individual station can be written as:

$$P(m) = \Phi\left(\frac{m - \mu}{\sigma}\right) \qquad (1)$$

Here, Φ is the cumulative distribution function of the standard normal distribution. The parameter μ is the 50% incremental detection threshold and σ is the standard deviation of the detection curve.

Figure 1. The source region selected for the case study presented here is centered on 32°N 104°E in China, having a radius of 1.5°, as shown by the open circle. The red curve shows the great circle path to the ARCES array in northern Norway, located at a distance of 56.4° from the center of the source region.

Denoting by D the ensemble of REB events of magnitudes m_i in this region detected by ARCES, we have the following likelihood function (Ringdal, 1975):

$$L(\mu, \sigma) = \prod_{i \in D} \Phi\left(\frac{m_i - \mu}{\sigma}\right) \prod_{i \notin D} \left(1 - \Phi\left(\frac{m_i - \mu}{\sigma}\right)\right) \qquad (2)$$

Here, the m_i are the network magnitudes of the events in the data set. The symbol μ is the ARCES 50% detection threshold for this region which will be estimated together with σ as the value which maximizes the likelihood

function (2). We choose to restrict σ to be within the range 0.10 - 0.60, since the estimation of this parameter can become unstable when the number of reference events is small. Figure 2 (top two panels) shows an example of application of *Method 1*.

Method 1 does not make use of all the relevant information provided by the IDC. This information includes the signal-to-noise (SNR) values for the detected phases, as well as noise levels for the non-detections (in certain cases). We now wish to use this additional information in order to estimate regional detection thresholds.

Method 2

We denote by *Method 2* the following approach, again using the ARCES case study as an illustration: For each REB event in this source area detected by ARCES, we scale down the network magnitude values by the log(SNR), to arrive at an instantaneous "noise magnitude". We then add 0.5 m_b units (corresponding to SNR~3) to obtain an estimate of the instantaneous ARCES detection threshold. By carrying out the procedure described above for all the detected events, we obtain a set of instantaneous thresholds, as shown as a function of magnitude in Figure 2 (third panel from top). We can calculate the mean and standard deviation of these values to obtain an estimate of the regional 50% threshold.

The instantaneous ARCES detection threshold a_i for the *i'th* detected event is thus:

$$a_i = m_i - \log(SNR_i) + 0.5 \tag{3}$$

If the number of detected events is *ND*, the estimate by *Method 2* then becomes:

$$\mu = \frac{1}{ND}\left(\sum_{i \in D} a_i\right) \tag{4}$$

A problem with this approach is that the instantaneous thresholds a_i estimated in this way turns out to be magnitude dependent. This is because of the influence of non-detections at low magnitudes. As can be seen from Figure 2 (top panel), the percentage of non-detections increases dramatically below magnitude 4.0. As a consequence, only those events with particularly favorable path focusing effects or unusually low noise levels at the time of the event would be detected, and thus estimating the thresholds solely on the basis of the detected events as done in *Method 2* would introduce a systematic bias.

Method 3

The problems mentioned for *Method 2* leads us to *Method 3*, which we summarize as follows. For each event undetected by ARCES we have the additional information that the instantaneous ARCES detection threshold in such cases must be higher than the corresponding magnitude value m_i of the reference network. We are thus faced with a classical maximum likelihood estimation framework. Specifically, we have a number of point estimates of the instantaneous ARCES detection threshold (for those events detected by ARCES), and a number of lower bounds (corresponding to the ARCES non-detections).

Thus, for $i \in D$ we have that

$$a_i < m_t < a_i + da_i \tag{5}$$

$$P(a_i < m_t < a_i + da_i) = \frac{1}{\sigma}\phi\left(\frac{a_i - \mu}{\sigma}\right)da_i \tag{6}$$

Here, ϕ is the density function of the standard normal distribution and *P* denotes probability.

Correspondingly, for $i \notin D$ we have that

$$m_t > m_i \tag{7}$$

$$P(m_t > m_i) = 1 - \Phi\left(\frac{m_i - \mu}{\sigma}\right) \tag{8}$$

We can then easily derive the likelihood function for *Method 3*, which becomes:

$$L(\mu, \sigma) = \prod_{i \in D} \frac{1}{\sigma}\phi\left(\frac{a_i - \mu}{\sigma}\right) \prod_{i \notin D} \left(1 - \Phi\left(\frac{m_i - \mu}{\sigma}\right)\right) \tag{9}$$

The symbol μ represents the ARCES 50% incremental detection threshold which we will estimate together with σ as the value which maximizes the likelihood function (9). As with *Method 1*, we choose to restrict σ to be in the interval 0.10-0.60.

We note in passing that the likelihood function (9) is similar to the one developed by Ringdal (1976), with the important difference that the non-detections here provide *lower bounds* rather than the *upper bounds* presented in that paper. Following the procedure described in that paper, we can derive an approximation of the standard deviation associated with the estimate of μ in (9). Assuming that σ is known, the variance Var (μ), (i.e., the square of the standard deviation) becomes:

$$Var(\mu) = \sigma^2\left[\sum_i \left(-y_i\phi(y_i) + \Phi(y_i) + \frac{[\Phi(y_i)^2]}{1 - \Phi(y_i)}\right)\right]^{(-1)} \tag{10}$$

where $y_i = (a_i - \mu)/\sigma$ for $i \in D$ and $y_i = (m_i - \mu)/\sigma$ for $i \notin D$

Figure 2 (bottom panel) shows the scaled-down thresholds for detected events as well as the lower limits for the non-detected events for the ARCES case study. Based on this information, we can estimate the overall ARCES detection threshold for the target site, using equation (9) which takes into account detections as well as non-detections. We obtain a threshold of 3.81, which is slightly higher than the threshold of 3.69 obtained by *Method 2*.

We note that for the case study discussed in this section, the three methods produce very similar threshold estimates (see Figure 2). The situation may be quite different in cases where fewer events are available for the estimation. A comparison of the three methods will be presented in the following.

Comparison of the estimation procedures

We proceed to compare the three methods for an extended dataset, comprising a large number of source regions, and we begin by comparing *Method 1* (Direct estimation using detection/no detection information only) and *Method 3* (MLE using scaled network magnitudes). Figure 3 (left panel) shows the results of such a comparison for the ARCES array, displaying the results for all the bins with at least 5 detected events and 5 undetected events, and where the standard deviation using *Method 1* is less than 0.4. The results are quite consistent, which is encouraging. We note that in cases when there are sufficient observations (like the case presented in the figure), *Method 1* and *Method 3* provide consistent results. We also note that *Method 3* uses more information and is therefore expected to be more stable when there are few observations.

We next compare *Method 2* and *Method 3*. Figure 3 (two right panels) shows the results for the ARCES array, again plotting all the bins with a sufficient number of observations. We note that the results are not as consistent as

between *Method 1* and *Method 3*, but that it is possible to improve the consistency by estimating and removing a linear trend.

We will use *Method 3* when the LEB contains information about non-detecting stations. For primary stations, such information is provided for distance range 20-100 degrees. Outside this distance range, we will use *Method 2*. For auxiliary stations, the LEB does not contain any information about non-detections before 2008, and in order to obtain consistency, we therefore chose to use *Method 2* for all auxiliary stations at all distance ranges.

Station detection capabilities

For the regionalized threshold estimates in this study, we make the following choices: For IMS primary stations, we use the maximum-likelihood estimate of the event detection thresholds *(Method 3*) in the distance range 20-100 degrees. Outside the 20-100 degree distance range we use the average scaled-down estimates *(Method 2*), but in addition, for each station, we calculate a regression line in order to estimate an average trend in a way similar to that illustrated in Figure 3 (upper right panel), and then compensate for this trend. For IMS auxiliary stations, we use *Method 2*, and compensate for a trend representing an average of those applied to the primary stations.

In Figures 4 and 5 we show, as an illustration, the results from applying this estimation procedure to primary station AKASG in Ukraine. In this study, we have applied the similar procedures to all available IMS primary and auxiliary stations, and the results form the basis for our application of dynamic phase information to assess the automatic IDC event lists.

Application to SEL event lists

We have developed a procedure for automatic application of the regionalized detection thresholds to assess the validity of individual candidate events in the SEL event lists as well as assess the consistency of individual phases associated with such events. We have applied this procedure to a large number of events, and for illustration we present an example of such application in Figure 6. The candidate event shown in this figure is typical of many of the false associations in SEL3, but it should be noted that the majority of the candidate events in SEL3 are real, and many of them have a remarkably accurate set of automatically associated seismic phases. Nevertheless, there is a clear need for improvement, and this project aims at providing a significant contribution in this regard.

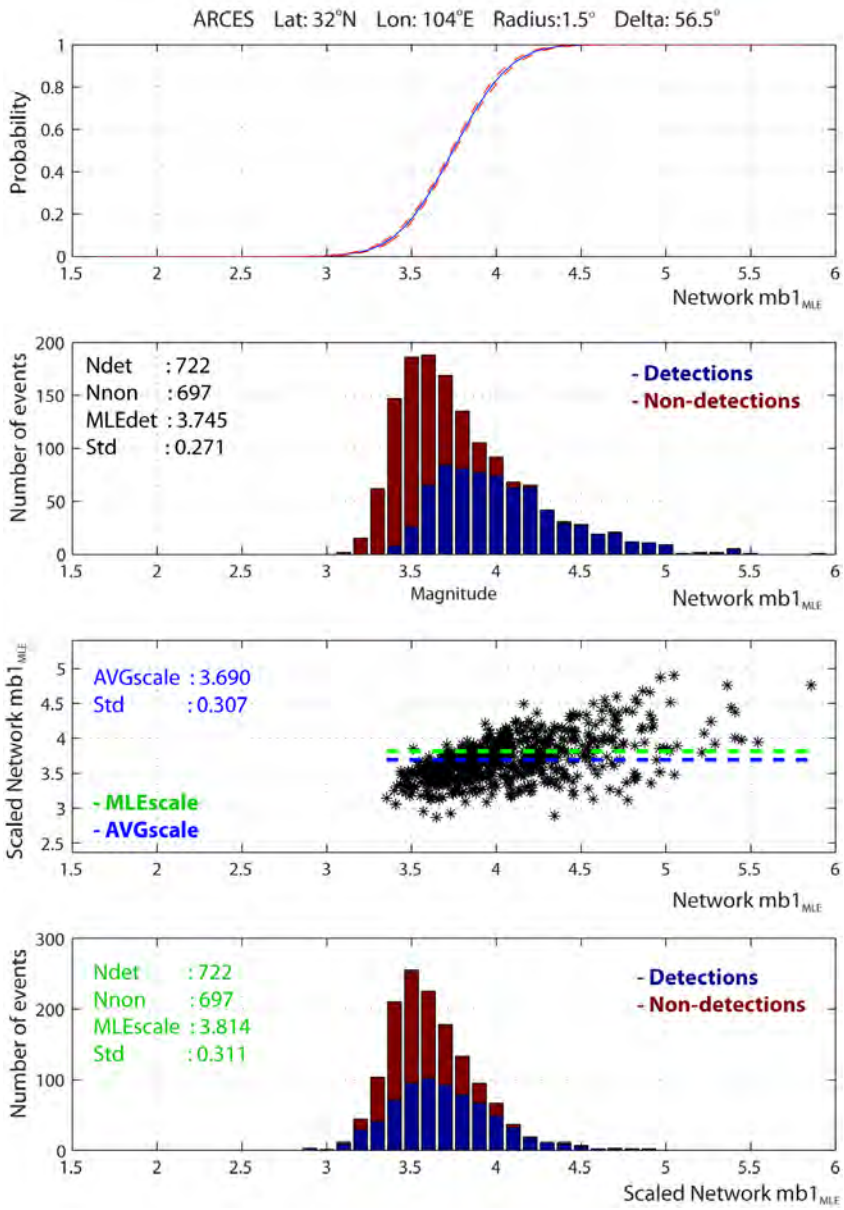

Figure 2. The three estimation methods, as applied to ARCES for the source region shown in Figure 1 all give similar results, as shown in this figure:

- ***Method 1* is illustrated in the top two panels. The station detection threshold (MLEdet) is given by the 50% level of the probability curve shown in the top panel. The information about event magnitudes, station magnitudes and noise magnitudes of non-detecting stations are shown in the second panel from the top.**
- ***Method 2* is illustrated in the third panel from the top, and shows the scaled-down thresholds for detected events (blue) as well as their average value (AVGscale, also in blue). For comparison, the results of *Method 3* (MLEscale) are shown in green color.**
- ***Method 3* is illustrated in the bottom panel, and shows the scaled-down thresholds for detected events (blue) as well as lower limits for the non-detected events (red) for the ARCES case study. By maximizing the formula (9) we obtain a mean (MLEscale) and standard deviation of the detection threshold as indicated on the figure.**

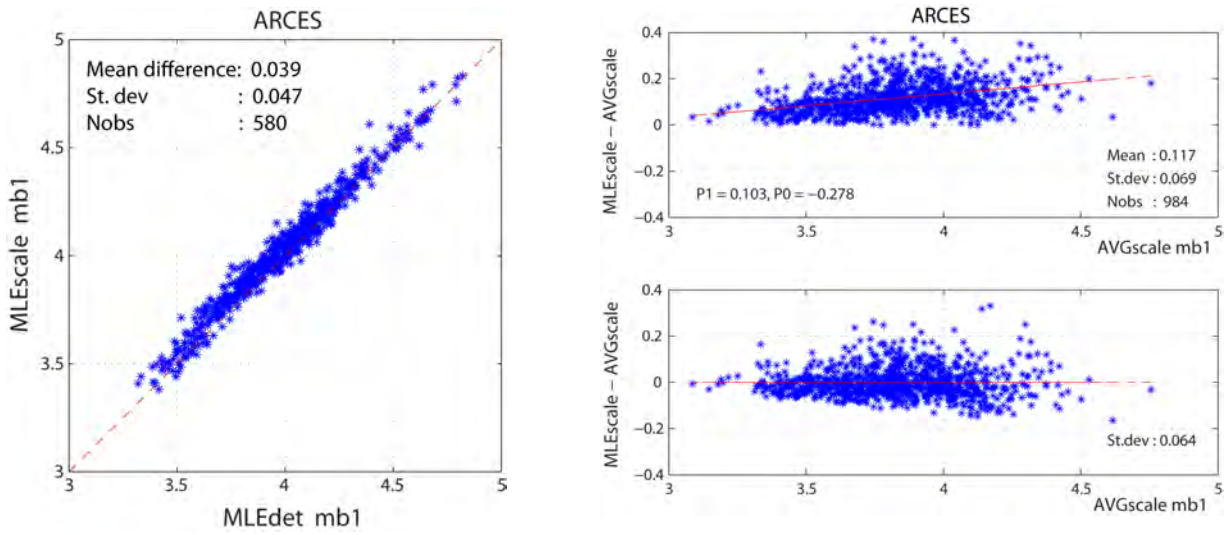

Figure 3. Comparison of the three estimation methods of event detection thresholds for IMS primary station ARCES:

Left panel: Correspondence between *Method 1* and *Method 3* estimates. The data represent 580 bins in the teleseismic distance range. The points on the plot represent all the bins (in a 2 by 2 degree grid) for which there are at least 5 detected events and 5 undetected events, and where the standard deviation of the detection curve using *Method 1* is less than 0.4. Results by *Method 1* (Direct estimation) are along the horizontal axis (MLEdet), while results by *Method 3* (MLE using scaled network magnitudes) are along the vertical axis (MLEscale).

Right panels: Correspondence between *Method 2* and *Method 3* estimates. The x-axis represents the event detection thresholds for different 2x2 degree bins using the average scaled-down magnitudes of events detected at ARCES. The y-axis shows the difference between the maximum-likelihood estimate (also taking into account non-detected events) and the scaled-down estimate. The top panel has a linear trend which is removed in the bottom panel.

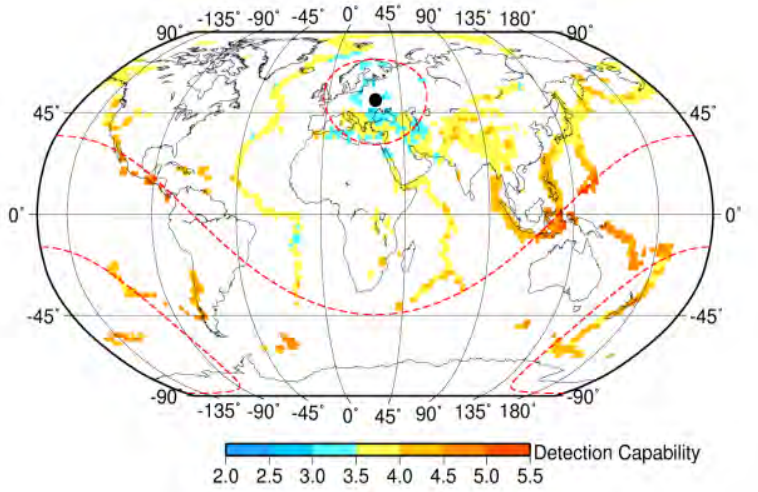

Figure 4. Maps showing the estimated regional event detection thresholds for IMS primary station AKASG. For each of the 2x2 degree bins, a minimum of 5 events are required for calculation of the detection threshold. The upper map shows a global projection, and distances of 20, 95 and 144 degrees from AKASG are illustrated by red dashed lines. The lower map shows an azimuthal projection, and the red dashed circle shows a distance of 20 degrees from AKASG.

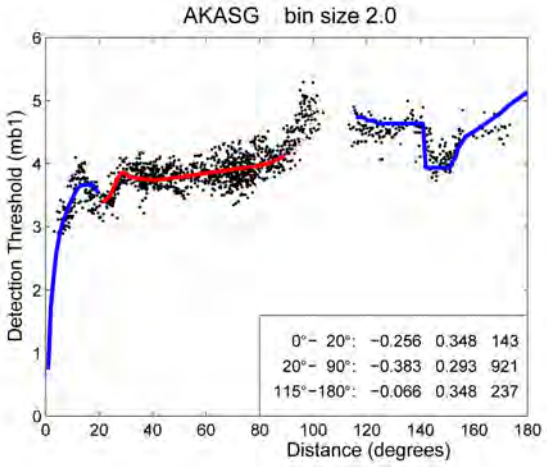

Figure 5. The black dots show the estimated regional event detection thresholds for IMS primary station AKASG plotted versus epicentral distance. For each of the distance ranges 0-20 degrees, 20-90 degrees, and 115-180 degrees, the mb1 amplitude-distance curve is fitted to the data. The numbers for each of the distance ranges, given in the lower right box, are:

1) **the constant offset level of the mb1 amplitude-distance curve,**
2) **the standard deviation, and**
3) **the number of bins.**

In general, the lower the constant offset level, the better is the overall station detection capability.

Northwest Africa										Event only in SEL3				
Event id	Year	Mo	Dy	Hr	Min	Sec	Lat	Lon	Depth	REB Lat	REB Lon	REB-SEL3 loc. diff	SEL3 mb	New mb_{MLE}
6828087	2010	11	10	03	24	24.400	7.17	-6.10	0.0f	-	-	-	4.23	3.54

Detecting stations							
Station	Phase	Delta	Event magnitude	Detection threshold	Sigma	Detection probability	Station magnitude
DBIC	Pg	1.33	3.5363	1.1059	0.4320	1.000000	-
PLCA	P	75.84	3.5363	4.3974	0.3000	0.002051	4.30
ULM	P	84.40	3.5363	4.4208	0.3090	0.002102	4.50
TXAR	P	93.08	3.5363	4.0911	0.3220	0.042467	3.90
Third highest detection probability						0.002102	
Lowest detection probability						0.002051	

Non-detecting operational IMS primary stations					
Station	Delta	Event magnitude	Detection threshold	Sigma	Detection probability
TORD	9.70	3.5363	2.9086	0.3000	0.981800
MKAR	83.73	3.5363	3.7313	0.3300	0.277324
FINES	59.18	3.5363	3.8318	0.3370	0.190282
BRTR	48.14	3.5363	3.8190	0.3000	0.173042
AKASG	52.37	3.5363	3.8287	0.3000	0.164861
GERES	44.78	3.5363	3.8528	0.3070	0.151312
YKA	92.09	3.5363	4.0508	0.4260	0.113574
ARCES	65.59	3.5363	4.0040	0.3740	0.105570
ZALV	84.80	3.5363	3.9853	0.3360	0.090752
LPAZ	65.64	3.5363	4.0100	0.3410	0.082410
ESDC	32.42	3.5363	3.9990	0.3120	0.069051
NOA	55.29	3.5363	4.0030	0.3000	0.059908
KBZ	56.13	3.5363	4.0293	0.3160	0.059384
WRA	139.62	3.5363	4.1460	0.3800	0.054315
ASAR	138.29	3.5363	4.1330	0.3620	0.049652
BOSA	46.69	3.5363	4.0929	0.3150	0.038626
GEYT	65.34	3.5363	4.0750	0.3000	0.036284
KEST	31.76	3.5363	4.2390	0.3460	0.021141
CPUP	59.80	3.5363	4.2120	0.3200	0.017361
BDFB	47.30	3.5363	4.1760	0.3000	0.016499
KMBO	44.03	3.5363	4.3623	0.3360	0.006981
SCHQ	67.56	3.5363	4.3396	0.3150	0.005388
MAW	88.74	3.5363	4.6437	0.3850	0.002011
ROSC	67.83	3.5363	4.5593	0.3340	0.001096
ILAR	102.56	3.5363	4.6168	0.3480	0.000952
KSRS	118.26	3.5363	4.8590	0.3970	0.000432
SONM	99.45	3.5363	4.6297	0.3160	0.000270
MJAR	125.17	3.5363	4.9410	0.3550	0.000038
CMAR	101.86	3.5363	4.9074	0.3420	0.000030
PETK	118.40	3.5363	5.0220	0.3650	0.000023
VNDA	109.40	3.5363	5.3630	0.4290	0.000010
NVAR	102.58	3.5363	4.9104	0.3000	0.000002
USRK	116.42	3.5363	5.1440	0.3370	0.000001
PPT	142.92	3.5363	5.5010	0.3000	0.000000
Number of primary non-detections:					34
Number of stations exceeding third detection probability					22
Number of stations exceeding lowest detection probability					22

Figure 6. This figure is an example of the type of processing results that we have obtained and analyzed for a large number of seismic events in SEL3. This particular example shows processing results from a candidate SEL3 event in Northwest Africa which has not been accepted in the LEB or REB. Three of the four detecting stations have a detection probability near zero. One non-detecting station (TORD) has a detection probability as high as 0.98. As many as 22 stations have better detection probability than the third best detecting stations. This event is clearly false, and can be discarded.

CONCLUSIONS AND RECOMMENDATIONS

We have developed a scheme to automatically process the individual candidate events in either SEL1, SEL2 or SEL3. For each event a set of consistency measures is calculated, as shown in the example in Figure 6. The consistency measures can be used individually or in combination. The most effective scheme is still to be developed.

In addition to calculating consistency measures based exclusively on SEL3 bulletin data, we have also during the developmental phase correlated the candidate events with the events actually accepted in the REB (or LEB). This provides a possibility to evaluate the consistency measures against the decision of the analyst.

In practical operation, it is intended to apply this processing scheme automatically, using the information from the SEL bulletins, the regionalized detection thresholds of the IMS stations, and the Threshold Monitoring (TM) results which are automatically computed at the IDC (see Kværna and Ringdal, 1999). We are already using the TM results to determine if any given station is actually in operation at a given time. Candidate events could be either accepted or rejected, or in some cases returned to the GA process for reanalysis, with one or more phases excluded from consideration.

Besides producing improved SEL lists, this processing scheme could also be applied in an interactive mode to provide the analyst with an assessment of the quality of the candidate event with respect to the pattern of detections/non-detections in view of the individual station capabilities.

REFERENCES

Kværna, T. and F. Ringdal (1999). Seismic Threshold Monitoring for Continuous Assessment of Global Detection Capability, *Bull. Seismol. Soc. Am*. 89: 946–959.

Kværna, T., F. Ringdal and U. Baadshaug (2009). Detection Capability of IMS Primary and Auxiliary Seimic Stations. *in* Semiannual Technical Summary, January-June 2009, *NORSAR Sci. Rep*. 2-2009, Kjeller, Norway.

Murphy, J. R. and B. W. Barker (2003). Revised Distance and Depth Corrections for Use in the Estimation of Short-Period P-Wave Magnitudes, *Bull. Seism. Soc. Am*. 93: 1746–1764.

Ringdal, F. (1975). On the estimation of seismic detection thresholds, *Bull. Seismol. Soc. Am*. 65: 1631–1642.

Ringdal, F. (1976). Maximum likelihood estimation of seismic magnitude, *Bull. Seismol. Soc. Am*. 66: 789–802.